ELSEVIER

Marine Geology 235 (2006) 177–192

MARINE GEOLOGY
INTERNATIONAL JOURNAL OF MARINE GEOLOGY, GEOCHEMISTRY AND GEOPHYSICS

www.elsevier.com/locate/margeo

Variability in cohesive sediment settling fluxes: Observations under different estuarine tidal conditions

Andrew J. Manning [a,b,*], Sarah J. Bass [b]

[a] *HR Wallingford, Estuaries and Dredging Group, Howbery Park, Wallingford, OX10 8BA, UK*
[b] *Centre for Coastal Dynamics and Engineering (C-CoDE), Coastal Processes Research Group, School of Earth, Ocean and Environmental Sciences, University of Plymouth, Portland Square Building (A504), Drake Circus, Plymouth, Devon, PL4 8AA, UK*

Accepted 3 October 2006

Abstract

The mass settling flux, which is defined as the product of the concentration and the settling velocity, is of prime importance with respect to both stratified and well mixed estuarine conditions. The determination of these fluxes (for applied modelling purposes) in high energy tidal estuarine environments, is very problematic. This is because the muddy sediments which dominate in estuaries, flocculate producing a variety of sizes and settling velocities, and this flocculation process is not understood well enough to be fully described theoretically. By drawing on examples of floc spectra acquired *in-situ* using the INSSEV system, this study explains how mass settling fluxes in the near-bed region can vary by three or four orders of magnitude in meso- and macro-tidal estuaries throughout a single tidal cycle. A floc population representative of dilute suspension conditions on a neap tide, indicated only 35% of the floc mass was macroflocs (>160 μm). However, the macrofloc settling velocity = 2.4 mm s^{-1}; three times faster than the microflocs, which meant the former fraction contributed 57% of the 205 mg $m^{-2}s^{-1}$ settling flux. Both highly concentrated (4–6 g l^{-1}) and very turbulent spring tide conditions (τ > 1.6 N m^{-2}) produced a bi-modal distribution in terms of the floc size and dry mass. With the former, 54% of the mass was contained within the 240–480 μm size fraction, with a further 25% of the dry floc mass in the flocs over 480 μm in diameter. These large flocs had settling velocities between 4–8 mm s^{-1}, which meant 99.5% of the settling flux (33.5 g $m^{-2}s^{-1}$) was accredited to the macroflocs. The high turbulence environment saw the dry floc mass distribution shift 60:40 in favour of the microflocs. The microfloc settling velocity was 1.45 mm s^{-1}, 0.35 mm s^{-1} faster than the larger macrofloc fraction. In terms of the total mass settling flux, 0.9 g m^{-2} s^{-1}, this translates into the microflocs contributing 70% during high turbulence. At slack water the flux only reached 12 mg m^{-2} s^{-1} and macrofloc growth was mainly attributed to differential settling. Continuous floc observations made over a complete tidal cycle revealed that the asymmetrical distribution of the tidal energy generated throughout the spring conditions in the Tamar estuary demonstrated a distinct control on the flocculation process. The less turbulent ebb produced 86% of the total tidal cycle mass settling flux, of which only 8% of the settling flux was outside the turbidity maximum. An attempt to simulate these large settling fluxes by using a constant settling rate of 0.5 mm s^{-1}, under-estimated the tidal cycle settling flux by 78%, with less than 15% of the total flux being estimated during the advection of the turbidity maximum on the ebb. In contrast, using a faster constant settling velocity parameter of 5 mm s^{-1}, (representative of the macrofloc fraction), resulted in a mass flux over-estimate of 116% for the tidal cycle duration.

Keywords: mass settling flux; flocculation; turbulent shear stress; settling velocity; effective density; INSSEV instrument

* Corresponding author. Tel.: +44 1752 232407; fax: +44 1752 232406.
E-mail address: andymanning@yahoo.com (A.J. Manning).

0025-3227/$ - see front matter © 2006 Elsevier B.V. All rights reserved.
doi:10.1016/j.margeo.2006.10.013

1. Introduction

Models of sediment transport are widely used as dredging management tools in estuarine locations. However an accurate representation of the vertical sediment settling fluxes is very problematic. This is due to the cohesive nature of the muddy sediments which dominate estuarial locations. Observations of fine sediment suspensions suggest that, except for extremely high energetic conditions, most of the sediment mass occurs as flocs (Kranck and Milligan, 1992). These cohesive sediments can flocculate to form a spectra of aggregates known as flocs. Flocs are less dense, but faster settling than their constituent particles. As flocs grow their effective density generally decrease, but their settling rates rise. Flocculation is a dynamically active process which readily reacts to changes in turbulent hydrodynamic conditions (Manning, 2001, 2004a). The flocculation of particles is a function of the mechanisms which bring the particles into contact, e.g. differential settling or turbulence (Manning and Dyer, 1999) and the mechanisms that make them stick together, e.g. salinity related electro-static charging or organic matter content (van Leussen, 1988). In addition to increasing particle collisions, turbulent shear may also break up aggregates (McCave, 1985), and this is further complicated by concentration gradients which can form in the near-bed region throughout a tidal cycle (Dyer et al., 2004).

The processes of aggregation and disaggregation are still not understood well enough to be fully described theoretically, and at the moment predictions tend to rely on empirical generalisations. Until recently, a lack of reliable floc measurements together with those of hydrodynamic turbulence, limited studies of the complex interactions between the factors affecting flocculation (e.g. shear, salinity, organic content and concentration) and floc characteristics. Laboratory experiments do not reliably represent field situations because of the difficulty of reproducing the chemical, physical and biological processes involved, and *in-situ* measurements have historically been unreliable because of floc disruption when sampling (van Leussen, 1988). However, the advent of video floc devices (e.g. van Leussen and Cornelisse, 1994; Hill et al., 1998; Mikkelsen et al., 2004), in particular the unique INSSEV instrument (Fennessy et al., 1994; Manning and Dyer, 2002) which was developed at the University of Plymouth (UK), and when combined with an array of miniature high frequency velocimeters, INSSEV has provided a means of accurately determining time series of both the spectral distribution of the floc dry mass and settling velocities, directly from within a turbulent estuarine water column. INSSEV has observed low density ($\sim$30 kg m^{-3}) macroflocs over 1.5 mm in diameter which have displayed settling velocities of 3–25 mm s^{-1} (Manning and Bass, 2004).

In contrast to floc particle sizers, the additional measurement of individual floc settling rates means that INSSEV can provide reliable estimates of floc effective density by using a modified Stokes' Law relationship. A knowledge of floc effective density is very important in the calculation of vertical settling fluxes (Manning, 2004b). As flocs increase in diameter they become more porous (>90–95%); since their voids are filled with interstitial water; the higher order flocs are less dense than the lower order microflocs. Very few direct quantitative studies have been conducted on floc effective density variations. Floc fragility has precluded the direct measurement of floc density. Also the rheological properties of suspended particulate matter are governed by volume concentrations, as opposed to mass concentrations (Dyer, 1989).

A flux which is of prime importance with respect to both stratified and well mixed estuarine conditions, is the mass settling flux (MSF), which is defined as the product of the suspended particulate matter (SPM) concentration and the settling velocity (Manning, 2004b). By drawing on examples of floc spectra acquired *in-situ* using the INSSEV system, this paper will illustrate in a semi-quantitative manner how these settling fluxes in the near-bed region can vary by three or four orders of magnitude in meso-/macro-tidal estuaries under different tidal conditions (Bass et al., 2006; Manning et al., 2006). The examples presented were obtained from experiments conducted in the Gironde Estuary, France and the Tamar Estuary, England, and cover a variety of conditions including: spring and neap tides, slack water and times when concentrations and turbulent shear stresses were high.

2. Method

2.1. Data acquisition

Near-bed flocculation dynamics during neap tides were studied in the lower reaches of the Gironde estuary during June 1999 as part of the European Commission (EC) funded SWAMIEE project international field experiment, referred to as *SWAMGIR1* (Manning et al., 2004). The sampling location was located 1 km from the shore at Le Verdon (3 km from the mouth) and this was within the vicinity of one of the localised mud deposits situated between Bordeaux and Talais (Jouanneau and Latouche, 1981). These 2–3 m deep patches of

cohesive sediment are significant to the estuary's sediment transport regime, as they move either landward or seaward in response to run-off.

Measurements during spring tide conditions were made in the mesotidal Tamar estuary as part of the EC funded COSINUS project in June and September 1998 (Berlamont, 2002), and an NERC-funded experiment in April 2003 (Bass et al., 2006). The Tamar estuary, which is topographically dendritic in shape, is located in south-west England and has numerous meanders and wide mud flats exposed at low water. The Tamar has a catchment of approximately 800 km^2, which is one hundred times smaller than the Gironde estuary. Data acquisition was conducted in a straight channel section in the upper Tamar estuary, within the tidal trajectory of the turbidity maximum (TM). For all experiments the instrumentation and data acquisition systems were similar and are described below.

Flocs, although stable in flowing turbulent water, easily break apart when sampled in response to additional shear created during acquisition (Eisma et al., 1997). Therefore, the floc populations presented in this paper were acquired at a nominal height of 0.5 m above the estuary bed, using the INSSEV — IN-Situ Settling Velocity-instrument (Fennessy et al., 1994). The INSSEV video system was used to measure floc size and settling velocity spectra. A unique feature of INSSEV is that the flocs are measured within a known volume of fluid, which permits the distribution of floc dry mass and floc porosity to be accurately estimated.

The sampling apparatus comprises two inter-connected chambers which allow flocs to be sampled directly from within a turbulent water column, whilst creating minimal disruption to the observed flocs. A high resolution monochromatic Pasecon tube miniature underwater video camera located in an aperture in the lower settling chamber wall viewed the settling flocs. The floc images were recorded by an analogue S-VHS video recorder which produces a practical lower resolution limit of 20 μm.

Detailed measurements of the near-bed hydrodynamical structure were gathered at an acquisition rate of 18 Hz (and low pass filtered at 5 Hz) using the POST — Profile Of Sediment Transport-system (Christie et al., 1997). The system consisted of four 2 cm diameter discus shaped electro-magnetic flow meters (EMCMs), and five optical back-scatter sensors (OBS). The EM sensors were arranged in pairs to measure the stream-wise u, cross-channel v, and vertical w components of the flow, at distances 0.25, 0.5 m and 0.75 m above the bed (depending upon the experiment). Changes in water depths were monitored using a Druck 2 bar absolute pressure transducer.

Vertical profiles of salinity, temperature and suspension concentrations were obtained every 15 min using a Seabird Systems SBE 19-03 CTD together with a Downing OBS. Corresponding velocity profiles through the water column were obtained using a Valeport 108 mk III impeller current meter. Peristaltic pumped water samples were obtained from 0.1 and 0.5 m above bed every half hour. Filtered samples were used to verify OBS and INSSEV estimates of suspended mass concentration, and to estimate the percentage of organic matter content by loss-on-ignition tests.

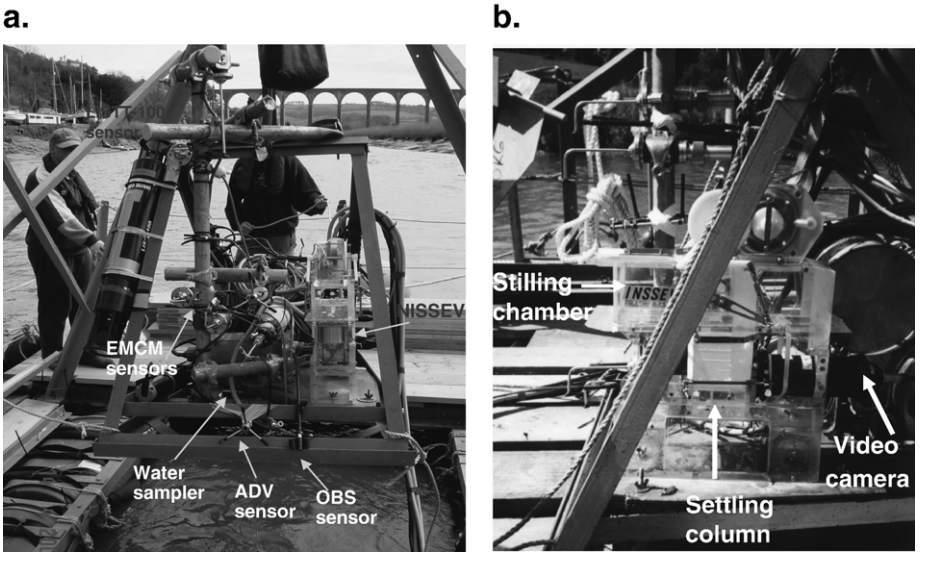

Fig. 1. INSSEV, EMCM, ADV and OBS sensors mounted on the estuarine bed frame — (a) front view and (b) side view.

INSSEV was mounted on a metal bedframe, whilst the POST sensors were attached to a vertical pole, which was positioned adjacent to the INSSEV sampling unit. Fig. 1 illustrates a typical instrumentation bed frame configuration awaiting deployment. To prevent vortex shedding occurring at the sampling orifice of the INSSEV stilling chamber, the rig was aligned to within ±5° with the dominant streamwise flow. This was achieved through the use of either control ropes attached to the outside of the frame and/or a rear fin (depending upon the estuarine location) to control orientation during lowering. A digital 2-axis tilt sensor and a fluxgate compass provided a direct readout of rig positioning on the estuary bed. The rig sat on the bed for the entire duration, sampling data from within an Eulerian reference frame.

2.2. Data processing

INSSEV flocs images were measured manually after each deployment from the video monitor, using size calibrations to convert the floc image to real dimensions. The two orthogonal floc dimensions which describe the floc shape (Dx and Dy), were converted into spherical-equivalent floc sizes (D).

By assuming that each floc is settling within the viscous Reynolds region (i.e. when the particle Reynolds number, R_e, <0.5–1), the effective density (ρ_e) for each floc could be obtained by applying a Stokes' Law relationship:

$$\rho_e = (\rho_f - \rho_w) = \frac{Ws18\mu}{D^2 g} \quad (1)$$

where: Ws is the floc settling velocity, μ the dynamic molecular viscosity and g is gravity. The effective density, also referred to as density contrast, is the difference between the floc bulk density (ρ_f) and the water density (ρ_w). The water density was calculated from measured salinity and water temperature data using the International Equation of State of Sea Water, 1980 (Millero and Poisson, 1981). Stokes' Law assumes that the settling particle is spherical, and observations have shown that flocs are often by no means spherical. Some of the large flocs have a very irregular shape, and are often joined into stringers by threads of biological matter (e.g. Eisma, 1986; Manning and Dyer, 2002). However, by direct measurement Alldredge and Gotschalk (1988) found that organic aggregates whose shape varied from spherical, including long comets, had settling rates very similar to those of nearly spherical particles. Similarly Gibbs (1985) showed that flocs from Chesapeake Bay had an average height:width ratios of to 1.6:1 which gave a spherical value of 0.91. Therefore, the implementation of a spherical equivalent diameter in Eq. (1) is valid.

Where the R_e exceeded 0.5, but was less than 2, the Oseen modification (Schlichting, 1968), as advocated by Brun-Cottan (1986) and Ten Brinke (1994), was applied to Eq. (1) in order to correct for the increased inertia created during settling. For instances where the R_e was greater than 2, the Schiller (1932) formula provides the best results. A series of algorithms was then applied to the INSSEV data from which dry floc mass and settling flux distributions were computed (Fennessy et al., 1997). This type of flux computational technique has also been applied successfully by: Syvitski et al. (1995), Hill et al. (1998), and Sternberg et al. (1999). Further details of the floc data processing are given in Manning (2004c).

Turbulent shear stress at the EMCM heights was estimated using the turbulent kinetic energy approach (e.g. Kim et al., 2000), which is less sensitive to sensor misalignment errors. Burst-averaged values of turbulent kinetic energy were calculated for each 227.5 s duration EMCM velocity data file.

3. Floc spectra

The first two floc spectra presented below are typically examples of average dilute suspension conditions (i.e. outside of the turbidity maximum zone) experienced during neap and spring tides when the flow was predominantly uniform and the lower region of the water column was generally well-mixed, with very little stratification present. The last three cases (3.3–3.5) will illustrate examples of floc populations present during the more extreme conditions experienced throughout a tidal cycle, including high concentration gradients, slack water and highly turbulent shear stress conditions, all of which can significantly affect the settling fluxes of cohesive sediments.

3.1. Neap tide flocs

Fig. 2 shows an example of a floc sample (G23-8) obtained during neap tides in the macro-tidal Gironde estuary (south-west France). Sample G23-8 was obtained 2 h and 10 min before high water, when the SPM concentration had risen to maximum of 139 mg l^{-1} and the turbulent shear stress was 0.46 N m^{-2}. The floc sizes ranged from 23 μm up to 362 μm, and these settled at velocities spanning three orders of magnitude from 0.04–3.4 mm s^{-1}. The diagonal lines on Fig. 2a

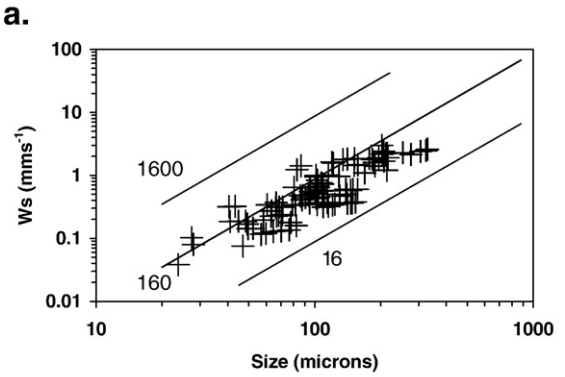

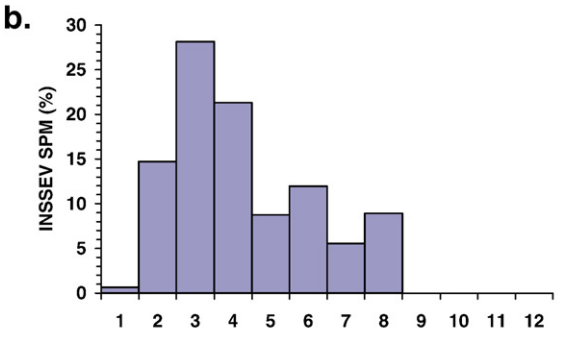

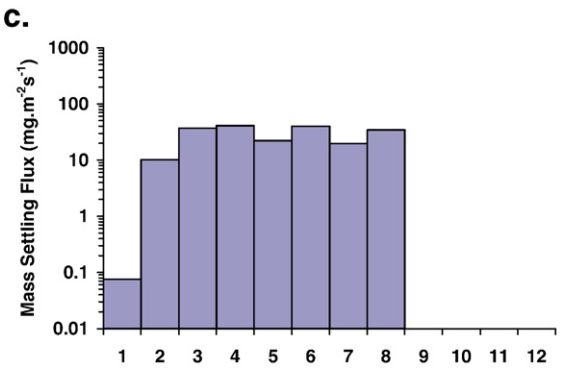

Size Band	1	2	3	4	5	6	7	8	9	10	11	12
Floc size (μm)	<40	40-80	80-120	120-160	160-200	200-240	240-320	320-400	400-480	480-560	560-640	>640

Fig. 2. Summary of floc characteristics for sample G23-8. Where (a) illustrates the relationships between floc size and settling velocities of individual flocs, with diagonal full lines showing the effective density (kg m^{-3}); (b) shows the size band distribution of SPM concentration; and (c) shows the mass settling flux spectrum.

illustrate contours of effective density (calculated by Eq. (1)) and indicate that there are many flocs of different sizes, but with the same density. Also there are flocs present with the same settling velocity, but exhibiting a wide range of sizes and densities. For G23-8, floc effective densities ranged between 40–812 kg m^{-3}. The shape of the largest macroflocs reflected a comet in appearance, with height to width ratios of 1.5–2.5. An example is shown in Fig. 3 by a macrofloc observed 79 s into the record (settling at 2.85 mm s^{-1}) with a Dx = 300 μm and Dy = 500 μm, and a corresponding effective density of 48 kg m^{-3}.

The flocs represented a total MSF of 205 mg $m^{-2}s^{-1}$. In terms of the SPM distribution (Fig. 2b), 86 microflocs (i.e. D < 160 μm) encompassed 65% of the floc mass, compared to just 20 individual macroflocs constituting the remaining 35%. However this translated into the macroflocs contributing 57% of the flux; a product of a

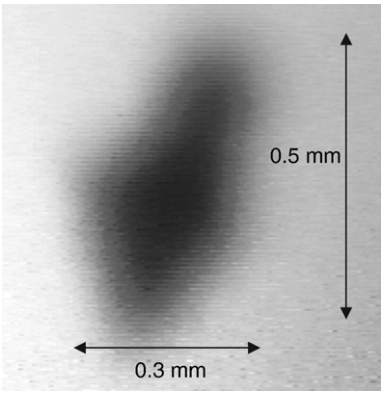

Fig. 3. A large low density "comet-shaped" macrofloc (sample G23-8, 79 s into record).

macrofloc (i.e. $D>160$ μm) settling velocity (Ws_{macro}) of 2.4 mm s^{-1}, which was three times faster than the Ws_{micro}. Similarly, the primary settling flux mode occurred in both the flocs 120–160 μm (Size Band (SB) 4) and 200–240 μm (SB6) in size; 40 mg $m^{-2}s^{-1}$ in each (Fig. 2c). The settling characteristics and ranges demonstrated by sample G23-8 are representative of neap tide floc populations typically encountered in dilute suspension conditions outside a turbidity maximum zone in many western European estuaries (Manning, 2004c).

3.2. Spring tide flocs

This spring tide example of a floc spectrum was measured during the COSINUS experiment in September 1998 in the Tamar Estuary (UK). Fig. 4 shows the record for INSSEV sample T21-1 which was collected on an ebb 2 h 10 min before low water. The particle concentration was much greater than the previous neap tide example, at just over 3 g l^{-1}, but with a similar shear stress (0.53 N m^{-2}) at the sampling height. As with the previous neap tide example, this sample was obtained outside of the turbidity maximum zone. Sample T21-1 constituted a total population of 750 individual flocs. There was a negative skewing of the population distribution across the size spectrum, with most aggregates having a near-spherical shape. Settling velocity distributions showed a very linear increase in settling rate, with each larger size band sub-group. The population was dominated by an abundance of macroflocs, with 77.6% of the mass contained by flocs in excess of 200 μm in size. The aggregates composing this section of the floc population became progressively less dense and more structurally porous, as their size increased. This tendency was shown by the respective values of effective density and porosity being 82 kg m^{-3} and 93.4% for the SB6 (200–240 μm) flocs. In comparison, the data revealed that the size band mean effective density for the flocs exceeding 640 μm in diameter had reduced to 25 kg m^{-3}, whilst the porosity had risen to 97.3%. Furthermore, the size spectrum showed that nearly half of the particulate mass was represented by flocs over 320 μm in diameter. It may also be hypothesised that the addition of a total carbohydrate concentration of 9.6 mg l^{-1} (Manning et al., 2006-this volume), which was 3.8 times higher than experienced during Tamar estuary neap tides, could have had a significant effect by assisting with inter-particular bonding as a result of the high collision frequency.

Although the spectrum showed a predominantly unimodal distribution of the SPM% (Fig. 4b), with a primary mode of 20.2% occurring at SB8 (320–400 μm), a much higher mass settling flux existed in the higher size bands despite their individually lower total mass content. For example, the largest size fraction (>640 μm) had a sub-population of 14 flocs and this constituted 4% of the total particulate mass in suspension, but with the aggregates possessing a mean settling velocity of 6.5 mms^{-1}, a resultant MSF of 820 mg $m^{-2}s^{-1}$ was attained (for SB12). Comparing this to the primary modal flux of SB8, which was a quarter of the total flux or 2860 mg $m^{-2}s^{-1}$, this fraction's settling flux contribution was 3.5 times greater than that attributed to the higher order SB12 flocs. However this was achieved by SB8 having 9.5 times as many floc comprising its sub-population. The total mass settling flux for this sample was 11.3 g $m^{-2}s^{-1}$. To put this into context, this MSF value was 6.7 times greater than the value computed by the use of an estimated settling velocity of 0.5 mms^{-1}; a typical parameterised Ws value used in numerical model simulation of sediment transport (J. Spearman, pers. com). Further general comments on applied modelling issues relating to Ws parameterisation and how it influences the settling flux will be made in Section 4.

3.3. Flocs formed in Concentrated Benthic Suspensions (CBS)

CBS layers form in the near-bed region, typically during the advection of a turbidity maximum. A main feature of a CBS is the turbulence damping which can occur within the layer as a result of density stratification; this can have a significant influence on the flocculation. Unlike a fluid mud, which acts independently from the main flow, a CBS is still transported with the dominant

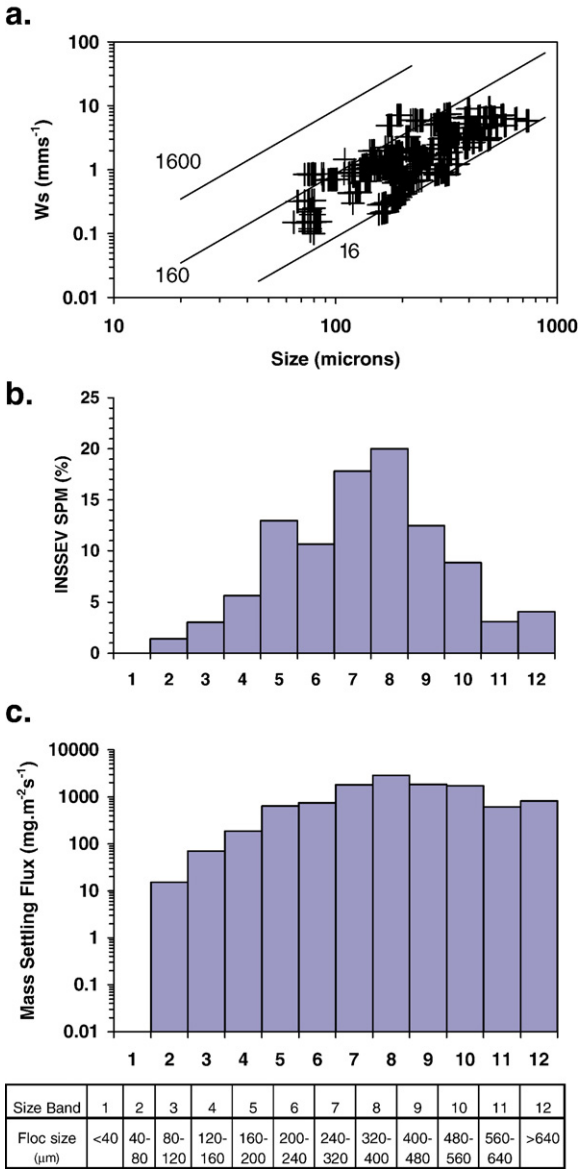

Size Band	1	2	3	4	5	6	7	8	9	10	11	12
Floc size (μm)	<40	40-80	80-120	120-160	160-200	200-240	240-320	320-400	400-480	480-560	560-640	>640

Fig. 4. Summary of floc characteristics for sample T21-1. Where (a) illustrates the relationships between floc size and settling velocities of individual flocs, with diagonal full lines showing the effective density (kg m^{-3}); (b) shows the size band distribution of SPM concentration; and (c) shows the mass settling flux spectrum.

current. The solids forming the CBS tend to be kept in suspension by turbulence, although the CBS layer can interact with the turbulent flow field. The CBS behaves as a Newtonian fluid, but with increased viscosity.

INSSEV sample T24-9 was acquired in September 1998 from within a Tamar estuary spring tide CBS layer of 5.6 gl^{-1}. The high concentration had restricted the turbulent energy to a shear stress of 0.36 Nm^{-2} at 0.5 m above the bed. This transformed the flocs into a bi-modal population in terms of the floc size and dry mass distribution (Fig. 5). Although the scatterplot showed a sub-group of slow settling ($Ws < 0.3$ mm s^{-1}) flocs in the 30–70 μm size range (Fig. 5a), these only constituted 9% of the total floc population. The majority of the particulate mass, 54%, was contained within the larger sized aggregates of SB7-9 (240–480 μm), with a further 25% of the dry floc mass contained in the three largest size bands (SB10-12). This cluster of large flocs had settling velocities between 4–8 mm s^{-1}, which produced a resultant mean settling velocity for the

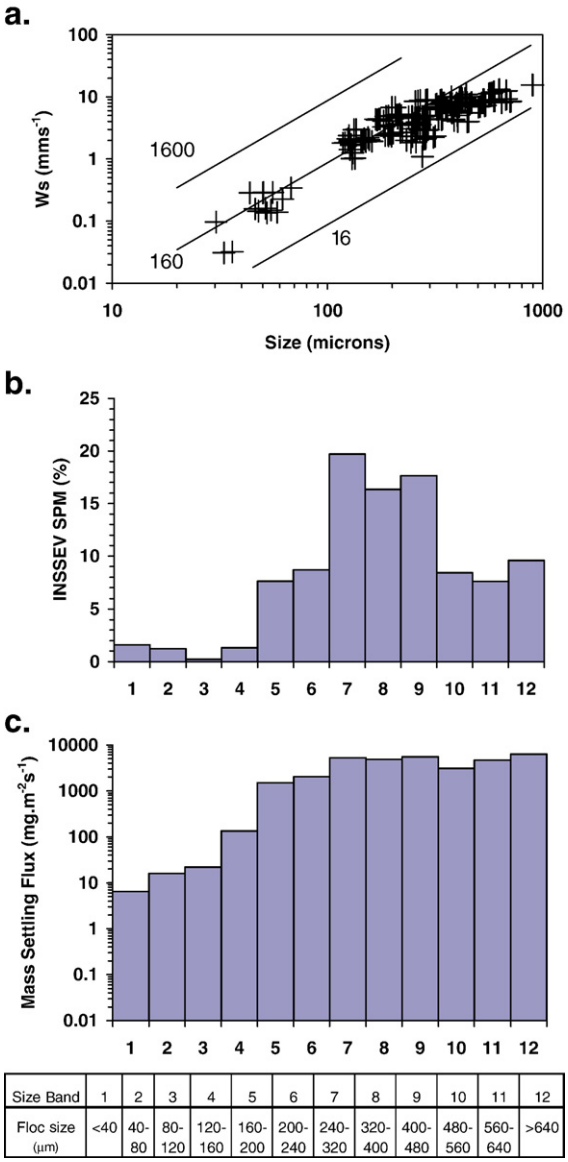

Size Band	1	2	3	4	5	6	7	8	9	10	11	12
Floc size (μm)	<40	40-80	80-120	120-160	160-200	200-240	240-320	320-400	400-480	480-560	560-640	>640

Fig. 5. Summary of floc characteristics for sample T24-9. Where (a) illustrates the relationships between floc size and settling velocities of individual flocs, with diagonal full lines showing the effective density (kg m^{-3}); (b) shows the size band distribution of SPM concentration; and (c) shows the mass settling flux spectrum.

fraction >160 μm of 5.7 mm s^{-1}, which was an increase of over 2.4 mm s^{-1} when compared to the earlier spring sample (i.e. T21-1). These macroflocs were on average 87% porous, with ρ_e predominantly <100 kg m^{-3}.

Of the 33.5 g $m^{-2}s^{-1}$ total MSF, 99.5% was accredited to the macroflocs (Fig. 5c). To put these values into perspective, this floc size spectrum which ranged from 30–894 μm represented a mass settling flux three times larger than typical Tamar spring tides outside of the CBS (T21-1) (Fig. 4), and 168 times greater than the Gironde neap tides example (G23-8). This highlights a significant optimisation in the flocculation present in CBS layers conditions. The high percentage of floc mass contained by the macroflocs situated within the TM was also observed by Dyer et al. (2002), and Manning et al. (2006).

3.4. Highly turbulent conditions

The second extreme condition examines a period in a tidal cycle when the turbulent energy dissipation attains a very high level. Such conditions were observed on a

flood in the Tamar estuary during a NERC funded experiment throughout high spring tides in April 2003 (Bass et al., 2006). The Tamar's topography creates a flood-dominant tidal asymmetry and a peak near-bed flood current velocity was attained just 2 h after low water. This generated a tidal cycle turbulent shear stress peak (at the INSSEV sampling height) of 1.62 N m^{-2}. Fig. 6 summarises how the 700 mg l^{-1} of suspended matter was distributed through floc sample T15-34. As with the CBS floc population, a dual modal floc population resulted, but with a reverse mass distribution to that observed during the optimum turbulent conditions of floc sample T24-9. The dry floc mass distribution was weighted 60:40 in favour of the microflocs (Fig. 6b). One can also see that the average settling velocity of the fraction greater than 160 μm was 1.1 mm s^{-1}, 0.35 mm s^{-1} slower than the microfloc fraction. In terms of the total mass settling flux, 0.9 g

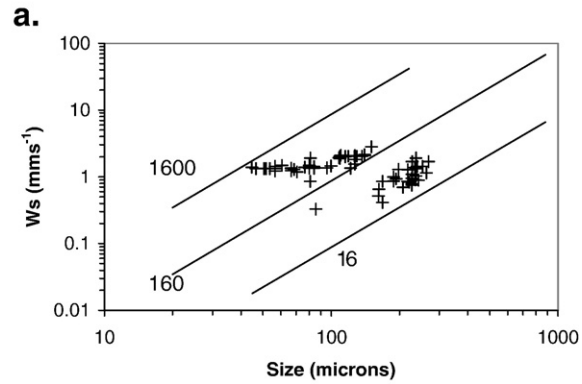

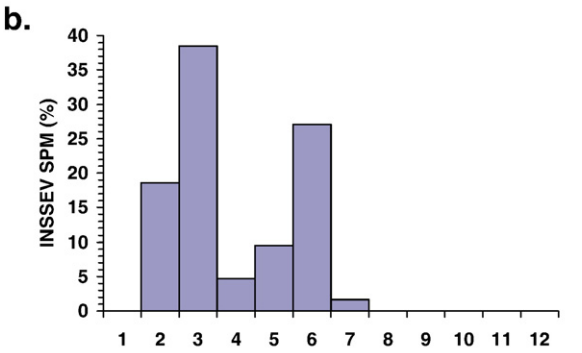

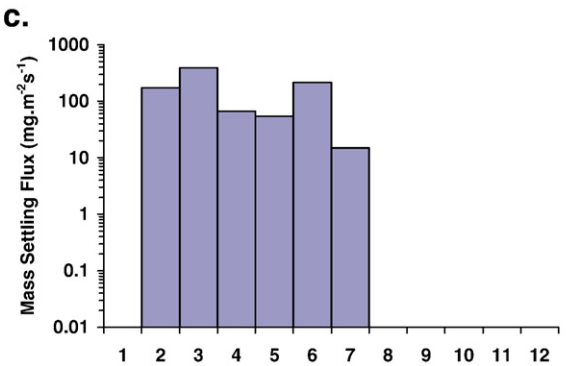

Size Band	1	2	3	4	5	6	7	8	9	10	11	12
Floc size (μm)	<40	40-80	80-120	120-160	160-200	200-240	240-320	320-400	400-480	480-560	560-640	>640

Fig. 6. Summary of floc characteristics for sample T15-34. Where (a) illustrates the relationships between floc size and settling velocities of individual flocs, with diagonal full lines showing the effective density (kg m^{-3}); (b) shows the size band distribution of SPM concentration; and (c) shows the mass settling flux spectrum.

m^{-2} s^{-1}, this translates into the microflocs contributing 70%.

The high microfloc settling velocities observed during sample T15-34 could be attributed to transitional de-aggregation of the macroflocs, from which these microflocs were probably the core sub-structure earlier in the tidal cycle. One could hypothesise that the fragile macroflocs, which tend to more readily interact with the turbulent dissipating eddies of a similar dimension, rapidly decrease in number with increasing shear stress. On reaching a shear stress in excess of about 1.5 N m^{-2}, only the most resilient macroflocs would remain intact.

The progressive de-flocculation which tends to occur in the water column with steadily rising near-bed shear stress, has therefore replaced the matter in suspension which was earlier held by a low number of large porous macrofloc flocs, with numerous higher density microflocs. The fragile, low density macroflocs attain equilibrium with the surrounding turbulence relatively quickly, typically the order of a few minutes. The smaller microflocs require a much longer duration to equilibrate with the water column turbulence than the macroflocs, as they demonstrate a greater resistance to break-up, a result of their stronger and closer internal bonds. Also, Manning (2004a) found that statistically the Ws_{micro} demonstrates a very close correlation with the turbulent energy dissipation present in the water column, whereas Ws_{macro} tends to be dependent on both turbulent shear and suspended particle concentration variations.

Results from a recent laboratory study (Gratiot and Manning, 2004) have shown that when microflocs are exposed to a more continued period of highly turbulent stimulation, microfloc fractions do eventually attain an equilibrium characterised by a slower average settling velocity than the macroflocs (within the same floc population). These findings agree with the residence time flocculation theory advocated by Winterwerp (1998). However, as will be demonstrated by the example in Section 4.1, the time scale of continued exposure by the flocs to very highly turbulent episodes during a tidal cycle in most European tidal estuaries, is significantly shorter than artificial laboratory simulations can create.

The INSSEV results showed that the T15-34 macroflocs settled 25% slower than the comparative microflocs. However, the macroflocs had a mean effective density of 41 kg m^{-3}, which was 12–13 times less dense than the smaller sized fraction. This, together with the video images, infers that the remaining macroflocs are stringy (height to width ratios up to 5), porous (85–90%), loosely-structured aggregates. With the organic content at the acquisition time being 40%, one can assume that these low density macroflocs are predominantly organically-based, possibly comprising strands of vegetation, in particular the macroalga *Enteromorpha* (Romano et al., 2003).

When such large velocity gradients develop close to the bed, the highly consolidated bed layer may erode. This can result in the entrainment of very strongly bonded microflocs, which have maintained their compositional history during deposition on an earlier tidal cycle. The degree to which microflocs in suspension are either the result of direct flocculation occurring whilst in suspension, or simply re-entrained aggregates, is a product of the bed consolidation processes, together with mineralogical and organic constituents which influence the microfloc bonding. However, the microfloc populations are ultimately controlled by the turbulent mixing.

3.5. Slack water conditions

In contrast to the highly turbulent scenario described previously, high water slack produces a quiescent water column with negligible mixing. Gironde estuary sample G23-19 was acquired when the SPM had fallen below 10 mg l^{-1} and the turbulent shear stress was only 0.06 Nm^{-2}. At this point in the tidal cycle, only 17 individual flocs were captured in sample G23-19 (Fig. 7a), and only two flocs had settling speeds greater than 1.5 mm s^{-1}. This implies that most of the G23-19 flocs were probably created higher in the water column, and with their lower rates of fall, it had taken longer for them to reach the sampling height.

The two thirds of the particulate mass were microflocs, however due to the slow settling rate of this fraction (Ws_{micro}=0.6 mm s^{-1}), the macroflocs represented nearly 70% of the total settling flux, which was 12 mg m^{-2} s^{-1}. Closer examination of the macroflocs shows that the two largest flocs (D=270 and 277 μm) were three times smaller than the corresponding Kolmogorov eddy size of 870 μm. These two macroflocs constituted 28% and 61% of the SPM and MSF, respectively. Possessing effective densities of less than 75 kg m^{-3} and fall velocities of 3 mm s^{-1}, these macroflocs may have been the product of particle scavenging through differential settling collisions which are only effective in relatively still water columns (Lick et al., 1993).

4. Settling flux time series

4.1. Main variables

Fig. 8 illustrates the salinity profile and water level changes (A) and suspension concentration and shear

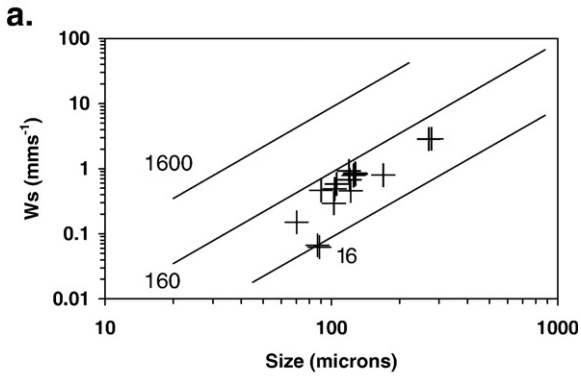

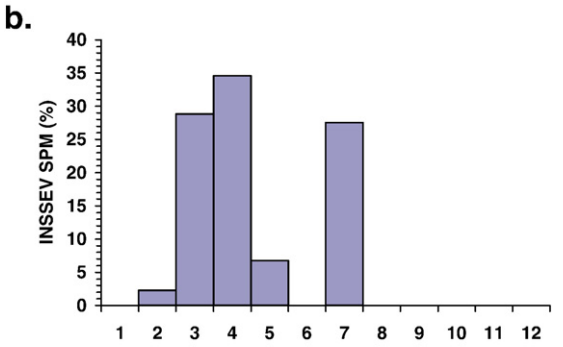

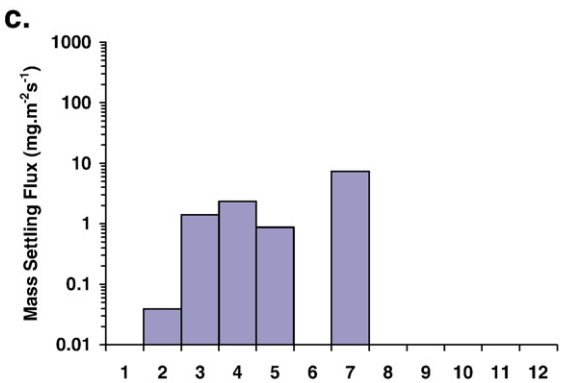

Size Band	1	2	3	4	5	6	7	8	9	10	11	12
Floc size (μm)	<40	40-80	80-120	120-160	160-200	200-240	240-320	320-400	400-480	480-560	560-640	>640

Fig. 7. Summary of floc characteristics for sample G23-19. Where (a) illustrates the relationships between floc size and settling velocities of individual flocs, with diagonal full lines showing the effective density (kg m^{-3}); (b) shows the size band distribution of SPM concentration; and (c) shows the mass settling flux spectrum.

stress (B), 0.5 m above the estuary bed, throughout a full tidal cycle during the April 2003 Tamar experiment. The experimental deployments commenced at 08:10 h, which was 2 h after predicted local high water on an ebb flow, and experienced high spring tidal conditions. The initial 4 m deep water column was partly stratified with a surface salinity of 4.7, gradually increasing to 12 in the proximity of the estuary bed (Fig. 8a). By 09:45 h the water column was fresh throughout for the latter stages of the ebb. The near-surface current attained an ebb velocity of about 0.8 m s^{-1} by 10:30 h and this coincided with a peak turbulent shear stress of ~1.5 N m^{-2} (Fig. 8b). SPM concentration rose in response to the accelerating flow and with the passage of the turbidity maximum reaching a maximum concentration of 4.2 g l^{-1} by 09:50 h. Further inspection of the complete OBS array showed that a concentrated benthic suspension layer had developed by ~9:15 h where the

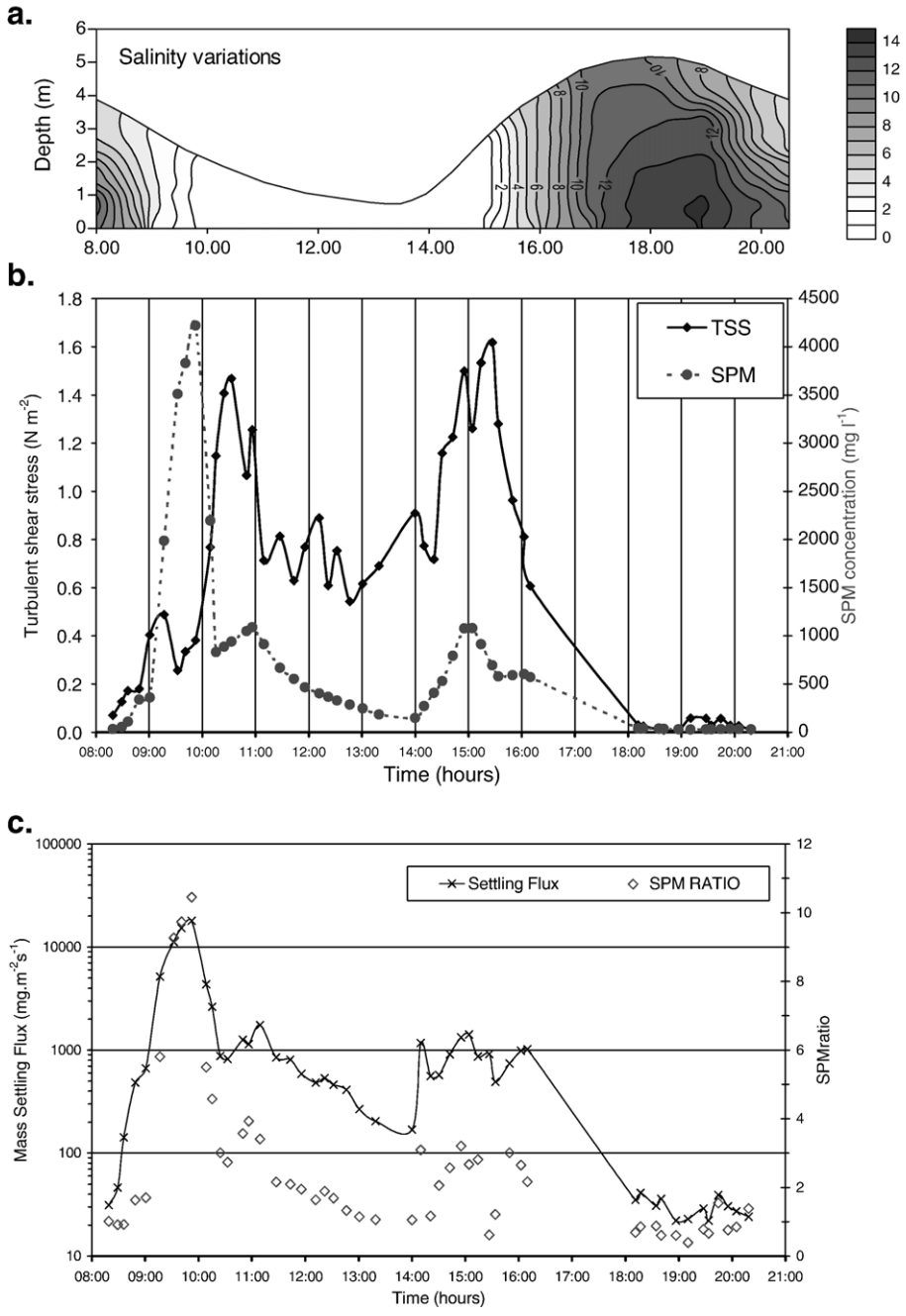

Fig. 8. Time series for the spring tide on the 15th April 2003 illustrating variations in: a. salinity, b. turbulent shear stress and suspended particulate matter concentration (data points are indicated), and c. mass settling flux and SPM ratio. Both b and c are observations at a constant 0.5 m above the bed.

lutocline rose to a height of 55–70 cm above the estuary bed and then dropped below the instrument height at ~10:15 h and persisted until 11:00 h (Bass et al., 2006). The suspended concentration rapidly decreased in the region above the lutocline. The formation of the CBS layer had the net effect of creating turbulence damping within the layer, and accounted for the observed reduction in turbulent shear within the CBS. Drag reduction (Best and Leeder, 1993; Manning et al., 2006) was also instigated at the lutocline. The asymmetric distortion in the tidal curve, primarily due to the estuary topography and the effects of tidal straining, were seen

to have prolonged the ebb beyond the predicted time of low water at 12:15 h by a further 1 h and 15 min.

The salt intrusion arrived at the sampling location on the flood as a well-mixed vertical wall at 15:45 h with a salinity of 2. The flood water advancement in the upper estuary had the appearance of a constant thickness saline layer pushing under a wedge of fresher water. A maximum surface flow velocity was achieved just over 1 h into the flood, and this was nearly double the peak velocity observed during the ebb. The maximum turbulent shear stress on the flood exceeded the peak ebb shear stress by 0.15 N m^{-2}. Initial observations suggested that the amount of particulate matter in suspension was severely restricted on the flood, with a near-bed concentration of only 1.1 g l^{-1} at 0.5 m recorded at 15:00 h. However, depth profiles of concentration revealed that the flood-dominant tide had mixed the suspended matter more evenly throughout the entire water column. By 19:00 h the near-bed salinity had increased to 14, reducing in the upper 1 m, to a salinity of 3 as the surface ebb current leads the start of the ebb at the bed. A more detailed study of the phase relationships which develop between the hydrodynamic activity and the entrained solids is reported in Bass et al. (2006).

4.2. Mass settling flux time series outputs

Fig. 8c illustrates how the MSF at 0.5 m varied through four orders of magnitude during the complete tidal cycle. A peak flux of 18 g m^{-2} s^{-1} occurred within the CBS layer during the ebb at 09:50 h. This very high flux was dominated by fast settling flocs; the average settling velocity of the macrofloc fraction was 4.3 mm s^{-1} and 0.94 mm s^{-1} was the corresponding microfloc settling rate.

A minimum MSF (0.015 g m^{-2} s^{-1}) was measured just after high water slack (19:10 h.). The main difference between the CBS and high water flux, was partly attributed to the significantly slower settling velocities of the flocs observed throughout the latter. At slack water the observed Ws_{macro} was more than four times slower than during the CBS, and the Ws_{micro} was only 0.42 mm s^{-1}, which is a 55% reduction in velocity.

The other factor which contributed to producing two significantly different mass fluxes, was the distribution of the floc mass at each instance. The most effective parameter which compares the distribution of particulate matter throughout the macrofloc and microfloc sub-populations, is the dimensionless SPM_{ratio} (Manning, 2004c) The SPM_{ratio}, which is also plotted on Fig. 8c, was calculated by dividing the percentage of SPM_{macro} by the percentage of SPM_{micro}. At periods of slack water the SPM_{ratio} was estimated as unity, which would represent an equal apportioning of the floc mass between the two floc sub-populations. Whereas the SPM_{ratio} was 12 within the turbidity maximum of the ebb, which equates to the macroflocs constituting 92.4% of the dry floc mass. The highly turbulent part of the flood, which favoured the microflocs, reduced the SPM_{ratio} to 0.66.

The more well mixed, turbulent flood produced settling fluxes of about 1 g m^{-2} s^{-1} for the period between 14:40–15:30 h, which was an order of magnitude lower than the corresponding mid-ebb settling flux. About 700 mg m^{-2} s^{-1} of the total flux was due to the faster settling microflocs. This is a complete reversal in macro-microfloc settling dynamics from the less turbulent mid-ebb.

In contrast to the high water period, high shear stress was present in the water column at low water slack and this meant that a high proportion of the orthokinetic inter-particle collisions would have only limited success in producing flocculation. The settling flux at low water was about 0.14 g m^{-2} s^{-1}, which placed it an order of magnitude above the high water slack conditions. The ratio of macrofloc to microfloc SPM was unity indicating an even distribution of floc mass through both sub-populations. The difference in settling velocity between the two fractions was only 0.4 mm s^{-1}, with the macrofloc having a settling velocity of 1.3 mm s^{-1}.

It must be noted that the settling flux is only an indication of the *potential* for deposition. The net settling flux is only part of the total vertical particle flux which consists of the settling flux and the turbulent entrainment flux. Depending on which one dominates, one has either deposition or entrainment.

5. Conclusions

During a representative dilute suspension neap tide floc population, only 35% of the floc mass was macroflocs. However the Ws_{macro}=2.4 mm s^{-1} was three times faster than the microfloc settling velocity. This meant the macroflocs contributed 57% of the 205 mg $m^{-2}s^{-1}$ settling flux.

Both highly concentrated (4–6 g l^{-1}) and very turbulent conditions (>1.6 N m^{-2}) produced a bi-modal distribution in terms of the floc size and dry mass. With the former, 54% of the mass was contained within the 240–480 μm, with a further 26% of the dry floc mass in the flocs over 480 μm in diameter. These large flocs had settling velocities between 4–8 mm s^{-1}, which meant 99.5% of the settling flux (33.5 g $m^{-2}s^{-1}$) was

accredited to the macroflocs. Whilst the high turbulence produced a 60:40 division in floc mass in favour of the microflocs. The microfloc settling velocity was 1.45 mm s^{-1}, 0.35 mm s^{-1} faster than the larger macrofloc fraction. In terms of the total mass settling flux, 0.9 g m^{-2} s^{-1}, this translates into the microflocs contributing 70%.

The asymmetrical distribution of the tidal energy generated throughout the spring tidal cycle in the Tamar estuary on 15th April 2003 demonstrated a distinct control on the flocculation process. The less turbulent ebb produced 86% of the total tidal cycle mass settling flux (at a constant 0.5 m above the bed), of which only 8% of the flux was outside the turbidity maximum. The accurate simulation of such large flux variations posses a distinct problem for numerical sediment transport modelling. For example, if a constant Ws of 0.5 mm s^{-1} was used (which is a settling velocity typically based on field settling tube gravimetric observations) to parameterise the settling flocs, this would have under-estimated the tidal cycle settling flux by 78%. Furthermore, less than 15% of the flux would have been estimated during the advection of the turbidity maximum on the ebb. However, if a faster constant settling rate is used, such as 5 mm s^{-1} (Petersen et al., 2002) which is solely representative of the macrofloc fraction, a flux over-estimate of 116% would result for the tidal cycle, but this reduced to a 48% over-estimated within the turbidity maximum passage.

Flocculation and flux spectra data sets, such as those presented in this paper, are required to correctly calibrate the depositional characteristics of estuarine muds in sediment transport models. There are significant dangers in basing a settling related parameterisation on data collected by instruments which are potentially more disruptive to a flocs fragile compositional integrity. Potential risks can also occur by taking the step of using a non-disruptive data acquisition technique to obtain empirical floc measurements, but then only utilising a very limited part of the total floc spectra, i.e. the fastest settling fraction, as the sole basis for representing spatial and temporal flocculation variations which are occurring in estuarine waters.

Laser diffraction particle sizers, such as the LISST – Laser In-Situ Scattering and Transmissiometry – (Agrawal and Pottsmith, 2000) and its derivatives, have recently become popular instruments with which marine scientist can measure floc size spectra in-situ, whilst creating minimum disruption to the flocs. However, a large number of western European estuaries are semi-diurnal and exhibit meso- to macro-tidal ranges which, as the data examples presented in this paper have shown, can entrain high concentrations of muddy sediments. Laser diffraction devices tend to saturate when the SPM concentration exceeds 400–500 mg l^{-1}. If this type of instrument was used to observe floc distributions over a tidal cycle, such as those measured by the INSSEV instrument during a spring tide in the Tamar estuary (refer to section 4), it would have missed 2.5 h on the ebb and 2 h on the flood due to sensor saturation. This translated into only 22% of the total MSF from the cycle being measured and as much as 89% of the flux generated during the passage of the turbidity maximum on the ebb (09:00–11:45 h) which could be lost. Furthermore particle sizers only provide measurements of floc size. Thus it is not possible to accurately assess either settling velocity or effective density variations, plus the dry mass distributions within a specific floc population; all of which have been seen to be both highly variable and important components for accurate flux parameterisation. Where as low intrusive video-based instruments such as INSSEV and LabSFLOC (the laboratory version), which can estimate floc effective density (through simultaneous size and settling velocity observations) of each individual floc from a population, provide a much more reliable floc monitoring solution. This is especially evident when studying settling fluxes within concentrated benthic suspension layers.

Acknowledgements

The author would like to thank the boat crews and all the technical staff who assisted during all the field experiments, in particular Peter Ganderton for his technical expertise. The Tamar estuary experiments were funded by both the European Commission MAST III programme as part of contract MAS3-CT97-0082 COSINUS (Prediction of cohesive sediment transport and bed dynamics in estuaries and coastal zones with integrated numerical simulation models) and the NERC under contract No.NER/M/S/2002/00108. The Gironde estuary was funded by the EC TMR SWAMIEE (Sediment and water movement in industrialised estuarine environments) project under contract No. ERBFMRXCT970111. The preparation of this paper was partially funded by HR Wallingford Ltd (UK), and the DEFRA/Environment Agency Joint Flood and Coastal Defence Research and Development Programme in Fluvial, Estuarine and Coastal Processes: Estuary Process Research (EstProc) project (under contract No. FD1905/CSA5966).

References

Agrawal, Y.C., Pottsmith, H.C., 2000. Instruments for particle size and settling velocity observations in sediment transport. Mar. Geol. 168 (1–4), 89–114.

Alldredge, A.L., Gotschalk, C., 1988. In-situ settling behaviour of marine snow. Limnol. Oceanogr. 33, 339–351.

Bass, S.J., Manning, A.J., Dyer, K.R., 2006. Preliminary findings from a study of the upper reaches of the Tamar Estuary, UK, throughout a complete tidal cycle: Part I. Linking sediment and hydrodynamic cycles. In: Maa, J.P.-Y., Sanford, L.P., Schoellhamer, D.H. (Eds.), Coastal and Estuarine Fine Sediment Processes-Proc. in Marine Science, vol. 8. Elsevier, Amsterdam. ISBN: 0-444-52238-7, pp. 1–14.

Berlamont, J.E., 2002. Prediction of cohesive sediment transport and bed dynamics in estuaries and coastal zones with integrated numerical simulation models. In: Winterwerp, J.C., Kranenburg, C. (Eds.), Fine Sediment Dynamics in the Marine Environment-Proc. in Mar. Sci., vol. 5. Elsevier, Amsterdam. ISBN: 0-444-51136-9, pp. 1–4.

Best, J.L., Leeder, M.R., 1993. Drag reduction in turbulent muddy seawater flows and some sedimentary consequences. Sedimentology 40, 1129–1137.

Brun-Cottan, J.C., 1986. Vertical transport of particles within the ocean. In: Buat-Menard, P. (Ed.), The Role of Air–Sea Exchange in Geochemical Cycling. D. Reidel Publishing Company, pp. 83–111.

Christie, M.C., Quartley, C.P., Dyer, K.R., 1997. The development of the POST system for in-situ intertidal measurements. The 7th Int. Conf. On Electrical Eng. in Oceanography, (London, England), Publication, vol. 439, pp. 39–45.

Dyer, K.R., 1989. Sediment processes in estuaries: future research requirements. J. Geophys. Res. vol. 94 (C10), 14327–14339.

Dyer, K.R., Bale, A.J., Christie, M.C., Feates, N., Jones, S., Manning, A.J., 2002. The turbidity maximum in a mesotidal estuary, the Tamar estuary, UK. Part II: the floc properties. In: Winterwerp, J. C., Kranenburg, C. (Eds.), Fine Sediment Dynamics in the Marine Environment — Proc. in Mar. Sci., vol. 5. Elsevier, Amsterdam. ISBN: 0-444-51136-9, pp. 219–232.

Dyer, K.R., Christie, M.C., Manning, A.J., 2004. The effects of suspended sediment on turbulence within an estuarine turbidity maximum. Estuar. Coast. Shelf Sci. 59, 237–248.

Eisma, D., 1986. Flocculation and de-flocculation of suspended matter in estuaries. Neth. J. Sea Res. 20 (2/3), 183–199.

Eisma, D., Dyer, K.R., van Leussen, W., 1997. The in-situ determination of the settling velocities of suspended fine-grained sediment — a review. In: Burt, N., Parker, R., Watts, J. (Eds.), Cohesive Sediments — Proc. of INTERCOH Conf. (Wallingford, England). John Wiley & Son, Chichester, pp. 17–44.

Fennessy, M.J., Dyer, K.R., Huntley, D.A., 1994. INSSEV: an instrument to measure the size and settling velocity of flocs in-situ. Mar. Geol. 117, 107–117.

Fennessy, M.J., Dyer, K.R., Huntley, D.A., Bale, A.J., 1997. Estimation of settling flux spectra in estuaries using INSSEV. In: Burt, N., Parker, R., Watts, J. (Eds.), Proc. of INTERCOH Conf. (Wallingford, England). John Wiley & Son, Chichester, pp. 87–104.

Gibbs, R.J., 1985. Estuarine flocs: their size settling velocity and density. J. Geophys. Res. 90 (C2), 3249–3251.

Gratiot, N., Manning, A.J., 2004. An experimental investigation of floc characteristics in a diffusive turbulent flow. In: Ciavola, P., Collins, M.B. (Eds.), Sediment Transport in European Estuaries. J. Coast. Res., SI, vol. 41, pp. 105–113.

Hill, P.S., Syvitski, J.P., Cowan, E.A., Powell, R.D., 1998. In situ observations of floc settling velocities in Glacier Bay, Alaska. Mar. Geol. 145, 85–94.

Jouanneau, J.M., Latouche, C., 1981. The Gironde estuary. In: Fuchtbauer, H., Lisitzyn, A.P., Milliman, J.D., Seibold, E. (Eds.), Contributions to Sedimentology, vol. 10. E. Schweizerbart'sche Verlagsbuchhandlung (Nagele u. Obermiller), Stuttgart, Germany. 115 pp.

Kim, S.-C., Friedrichs, C.T., Maa, J.P.-Y., Wright, L.D., 2000. Estimating bottom stress in tidal boundary layer from acoustic Doppler velocimeter data. J. Hydraul. Eng. 126 (6), 399–406.

Kranck, K., Milligan, T.G., 1992. Characteristics of suspended particles at an 11-hour anchor station in San Francisco Bay, California. J. Geophys. Res. 97, 11373–11382.

Lick, W., Huang, H., Jepsen, R., 1993. Flocculation of fine-grained sediments due to differential settling. J. Geophys. Res. 98 (C6), 10,279–10,288.

Manning, A.J., 2001. A study of the effects of turbulence on the properties of flocculated mud. Ph.D. Thesis. Institute of Marine Studies, University of Plymouth, 282p.

Manning, A.J., 2004a. The observed effects of turbulence on estuarine flocculation. J. Coast. Res., SI 41, 90–104.

Manning, A.J., 2004b. The development of new algorithms to parameterise the mass settling flux of flocculated estuarine sediments. Technical Report, vol. TR 145. HR Wallingford Ltd., England. 26 pp.

Manning, A.J., 2004c. Observations of the properties of flocculated cohesive sediment in three Western European estuaries. J. Coast. Res., SI 41, 70–81.

Manning, A.J., Bass, S.J., 2004. Experimental and predictive modelling observations of cohesive sediment settling fluxes in high energy tidal estuarine environments. In: Bartholdy, J., Pedersen, J.B.T. (Eds.), Proc. 6th Int. Conf. on Tidal Sediments, Tidalites Book of Abstracts, Uni. Copenhagen, pp. 128–129.

Manning, A.J., Dyer, K.R., 1999. A laboratory examination of floc characteristics with regard to turbulent shearing. Mar. Geol. 160, 147–170.

Manning, A.J., Dyer, K.R., 2002. The use of optics for the in-situ determination of flocculated mud characteristics. J. Optics A: Pure and App. Optics, vol. 4. Institute of Physics Publishing, pp. S71–S81.

Manning, A.J., Dyer, K.R., Lafite, R., Mikes, D., 2004. Flocculation measured by video based instruments in the Gironde Estuary during the European Commission SWAMIEE project. J. Coast. Res., SI 41, 58–69.

Manning, A.J., Bass, S.J., Dyer, K.R., 2006. Preliminary findings from a study of the upper reaches of the Tamar Estuary, UK, throughout a complete tidal cycle: Part II. In-situ floc spectra observations. In: Maa, J.P.-Y., Sanford, L.P., Schoellhamer, D.H. (Eds.), Coastal and Estuarine Fine Sediment Processes — Proc. in Marine Science, 8. Elsevier, Amsterdam. ISBN: 0-444-52238-7, pp. 15–33.

Manning, A.J., Bass, S.J., Dyer, K.R., 2006-this issue. Floc Properties in the Turbidity Maximum of a Mesotidal Estuary During Neap and Spring Tidal Conditions Mar. Geol. 235, 193–211, Tidalites S.I. (this volume). doi:10.1016/j.margeo.2006.10.014.

McCave, I.N., 1985. Mechanics of deposition of fine-grained sediments from nepheloid layers. Geo Mar. Lett. 4, 243–245.

Mikkelsen, O., Milligan, T., Hill, P., Moffatt, P., 2004. INSSECT — an instrumented platform for investigating floc properties close to the bottom boundary layer, Limnol. Oceanog. Methods 2, 226–236.

Millero, F.J., Poisson, A., 1981. International one-atmosphere equation of state seawater. Deep-Sea Res. 28, 625–629 (A).

Petersen, O., Vested, H.J., Manning, A.J., Christie, M.C., Dyer, K.R., 2002. Numerical modelling of mud transport processes in the Tamar Estuary. In: Winterwerp, J.C., Kranenburg, C. (Eds.), Fine sediment dynamics in the marine environment. . Proc. in Mar. Sci., vol. 5. Elsevier, Amsterdam. ISBN: 0-444-51136-9, pp. 643–654.

Romano, C., Widdows, J., Brinsley, M.D., Staff, F.J., 2003. Impact of *Enteromorpha* on near-bed currents and sediment dynamics: flume studies. Mar. Ecol., Prog. Ser. 256, 63–74.

Schiller, L., 1932. Flow in pipes. Handbook of Experimental Physics, vol. 4, Pt. 4. Academic Press, Leipzig, Germany, pp. 189–192.

Schlichting, H., 1968. Boundary-Layer Theory. McGraw-Hill, New York. 747pp.

Sternberg, R.W., Berhane, I., Ogston, A.S., 1999. Measurement of size and settling velocity of suspended aggregates on the northern California continental shelf. Mar. Geol. 154, 43–53.

Syvitski, J.P.M., Asprey, K.W., LeBlanc, K.W.G., 1995. In-situ characteristics of particles settling within a deep-water estuary. Deep-Sea Res. II 42, 223–256.

Ten Brinke, W.B.M., 1994. Settling velocities of mud aggregates in the Oosterschelde Tidal basin (The Netherlands), determined by a submersible video system. Estuar. Coast. Shelf Sci. 39, 549–564.

van Leussen, W., 1988. Aggregation of particles, settling velocity of mud flocs: a review. In: Dronkers, J., van Leussen, W. (Eds.), Physical Processes of Estuaries. Springer, Berlin, pp. 347–403.

van Leussen, W., Cornelisse, J.M., 1994. The determination of the sizes and settling velocities of estuarine flocs by an underwater video system. Neth. J. Sea Res. 31 (3), 231–241.

Winterwerp, J.C., 1998. A simple model for turbulence induced flocculation of cohesive sediment. J. Hydraul. Eng. 36 (3), 309–326.